Adaptive Online Power Management for More Electric Aircraft With Hybrid Energy Storage Systems

Yu Wang, *Member, IEEE*, Fang Xu, Shiwen Mao, *Fellow, IEEE*, Shanshui Yang, *Member, IEEE*, and Yinxing Shen

***Abstract*— More electric aircraft (MEA) has become the trend of future advanced aircraft for its potential to be more efficient and reliable. The optimal power management, thus, plays an important role in MEA, especially when using hybrid energy storage systems (HESSs). In this article, we propose a novel adaptive online power management (AOPM) algorithm for MEA, which aims to minimize the power fluctuation of the generators based on the battery–supercapacitor HESS. The problem is first formulated as a constrained stochastic programming problem. We then present an online algorithm to approximately solve the problem using the Lyapunov optimization method, which does not require any statistics and future knowledge of the electricity demand. We further propose the AOPM algorithm for MEA by incorporating an adaptive strategy with the online algorithm. Trace-driven simulation results demonstrate the effectiveness, efficiency, and adaptability of the proposed power management algorithm for MEA.**

***Index Terms*— Aircraft power systems, energy management, Lyapunov methods, power distribution.**

NOMENCLATURE

Symbol	*Description*
AOPM	Adaptive online power management.
BESS	Battery energy storage system.
ESD	Energy storage device.
ESS	Energy storage system.
HESS	Hybrid energy storage system.
MEA	More electric aircraft.
OPMA	Online power management system.
SC	Supercapacitor.
SOC	State-of-charge.

$R_k(t)$	Recharging power for ESD k in time slot t.
$D_k(t)$	Discharging power for ESD k in time slot t.
$R_{k,\max}$, $D_{k,\max}$	Maximum recharging power and maximum discharging power for ESD k.
$\eta_{k,r}$	Charging efficiency coefficient of ESD k.
$\eta_{k,d}$	Discharging efficiency coefficient of ESD k.
$E_k(t)$	Energy level of ESD k in time slot t.
$E_{k,\max}$, $E_{k,\min}$	Maximum and minimum capacity of ESD k.
$P_i^G(t)$	Output power for generator i in time slot t.
$P_{i,\max}^G$, $P_{i,\min}^G$	Maximum and minimum output power for generator i in time slot t.
$P^L(t)$	MEA load demand in time slot t.
$X_k(t)$	Virtual queue of ESD k in time slot t.
β_k	Shift parameter between E_k and X_k.
V, $V_{\max}$	Trade-off parameter and maximum trade-off parameter.
$\mathrm{SOC}_k(t)$	SOC of ESD k in time slot t.
$g(t)$	Power difference between the load and the generator output power.
f^{opt}	Optimal objective value for problem (7).
f^*	Optimal objective value for problem (16).
$\hat{f}$	Optimal objective value for problem (18).
α	Set parameter about the charging alert of SC.

Manuscript received September 24, 2019; revised December 25, 2019 and February 28, 2020; accepted March 31, 2020. Date of publication April 15, 2020; date of current version October 30, 2020. This work was supported in part by the Fundamental Research Funds for the Central Universities of China under Grant XCA17003-06 and in part by the U.S. National Science Foundation (NSF) under Grant DMS-1736470. *(Corresponding author: Yu Wang.)*

Yu Wang, Fang Xu, and Shanshui Yang are with the Department of Electrical Engineering, Nanjing University of Aeronautics and Astronautics, Nanjing 211106, China (e-mail: yuwang15@nuaa.edu.cn; fang.x@nuaa.edu.cn; yshanshui@nuaa.edu.cn).

Shiwen Mao is with the Department of Electrical and Computer Engineering, Auburn University, Auburn, AL 36830 USA (e-mail: smao@ieee.org).

Yinxing Shen is with Ningbo Power Supply Company, Zhejiang Electric Power Corporation of State Grid, Ningbo 315000, China (e-mail: xubanqiu@163.com).

Digital Object Identifier 10.1109/TTE.2020.2988153

I. INTRODUCTION

SINCE the 1940s, aircrafts have been using a combination of three secondary energy sources: hydraulic, pneumatic, and electric energy. This complex structure requires much effort to maintain high energy efficiency and system reliability. In response to these challenges, the MEA relying on more electrical power is proposed and becomes a popular trend for future aircrafts, which brings about significant benefits in reliability, maintainability, and survivability [1]–[3]. MEA also attracts many recent research interests on MEA system control [4], MEA electrical power system design [5], power system stability analysis [6], and also energy management [7].

In MEA, ESS is an important component, which is able to support power supply, absorb power load, and, thus, adjust the power balance inside the MEA power system. To make it work more effectively and efficiently, energy management is considered to be necessary for MEA. Several energy management methods have been developed to reduce load shedding, which is common in traditional control of the aircraft's power system but may be harmful to the stability of the system [8], [9]. New energy management solutions are then found to reduce or even avoid load shedding through the use of BESSs [10]–[12]. BESS is a kind of commonly used ESS composed of pure batteries, which has a long life, good economy, large energy density, high energetic efficiency, and low autodischarging rate [13]. However, BESS is not suitable for situations where load fluctuation is large because its power density is small. In some phases of MEA, such as the take-off, landing, and combat phases, the load pulse is about dozens of times of the average power, and it is, thus, very difficult for BESS to completely fulfill these power peaks unless its capacity is sufficiently large. However, the increase in capacity also leads to an increase in weight, which degrades the system's overall efficiency. To address this problem, different forms of ESS have been explored [7], [14]–[16], among which the HESS, consisting of batteries and SC, has obvious advantages over the others for MEAs. Since SC has a very high power density and discharges very fast [17], [18], it is complementary for batteries of small power density but large energy capacity.

On the other hand, power flows of HESS in the MEA power system may cause undesired voltage variations in the power bus. Some control strategies are, thus, proposed to address this problem. Li and Zhou [19] designed a control strategy according to different voltage states when the load is suddenly added and unloaded in the MEA power system. The work in [20] adopts fuzzy control methods to design a three-level control strategy to achieve voltage stability of MEA with HESS. Chen and Song [7] proposed a decentralized energy management strategy that splits the load power automatically into low- and high-frequency components and allocates them to HESS consisting of fuel cells and SC. Besides the power control, it is also possible to optimally schedule the charging and discharging of HESS to achieve better performance on power load absorption and power generation smoothness. Unfortunately, few works are found on the aspect of power optimization in MEA power management, which is fairly common in some other power systems with similar structures, such as the microgrid [21]–[23] and electric vehicles (EVs) [24], [25].

The work in [25] formulates a multiobjective optimization to optimize the power split in order to prolong the battery lifetime and to reduce the HESS power losses in EVs, and the problem is numerically solved online using dynamic programming. Zhou and Sun [22] proposed an improved particle swarm optimization (PSO) algorithm to solve the optimization problem, which takes one-time investment and the operation cost in the whole life cycle of HESS as the objective in a microgrid system. The article [23] proposes a hierarchical control architecture to optimize the power efficiency of the MicroGrid where the high-level power management controller solves an optimization problem by using model predictive control (MPC) controller to provide power references, while the low-level controller translates the power reference provided into a voltage or current level. It can be seen that these power management methods work to optimize the power flows inside a power system with HESS to achieve different objectives, such as power load smoothing, power loss minimization, and power efficiency maximization. The successful applications of these methods in similar power systems enlighten us to explore new power optimization schemes in the MEA power system to incorporate HESS more effectively and efficiently. However, the characteristics of the MEA power system also have some special requirements on the power optimization method, which also causes many difficulties. The methods well established in some other systems may not work well for MEA. For example, the abovementioned PSO and MPC are not applicable, as some power loads in MEA occur as nonlinear pulses, which cannot be predicted under any kind of model. It is, therefore, meaningful but challenging to develop power optimization for the MEA power system.

Motivated by this, we propose an MEA power management method based on the Lyapunov optimization approach in this article, which smooths the output power of the main generators by fully utilizing HESS to balance the power generation, power storage, and power loads, especially the pulses, in different flight phases of MEA. More importantly, it operates in an online manner. We choose to smooth the output power of the main generators because it limits the maximum output power, reduces the weight of the generators, and makes it easier to control and stabilize the voltage of the power bus. It also reduces the voltage and current stress on the devices and, thus, reduces fuel consumption, increases the stability of the MEA power system, provides better protection, and improves overall energy efficiency [24], [26], [27].

We first formulate a stochastic optimization problem to minimize the fluctuations of the output power of the generators under several constraints. The problem is solved using a Lyapunov optimization approach, which is effective at solving stochastic optimization and stability problems [28], [29]. We, in the following, introduce the energy storage virtual queues to transform the problem into a queue stability problem. The online solutions are also presented with the proof of several deterministic performance bounds. The algorithm is online since it only relies on the current system status and does not need any future knowledge on load demand. We then propose the AOPM scheme for MEA by further incorporating a control strategy with online power management, which is adaptive to load pulses. Finally, we perform trace-driven simulations to show that the proposed power management scheme can smooth the output power of the generators and is adaptive to load pulses. We also evaluate our proposed method under different HESS configurations to demonstrate its adaptability and effectiveness.

The remainder of this article is organized as follows. We formulate the problem in Section II. We propose the online solutions in Section III and then the adaptive online energy management scheme for MEA in Section IV. Section V

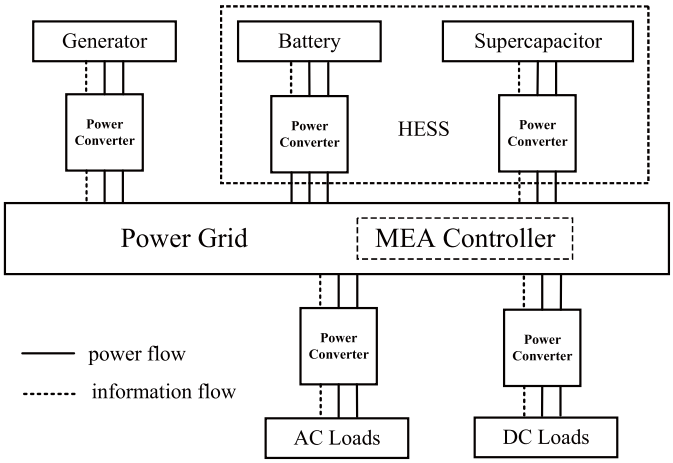

Fig. 1. MEA power system.

presents our simulation study, and Section VI concludes this article.

II. System Model and Problem Formulation

A. System Model

A typical MEA power system, as shown in Fig. 1, mainly consists of the power bus, main generators, HESS, power loads, and MEA controller. This system model is adaptable to both ac and dc power buses, according to the specific aircraft system, in which the main generators produce electrical power in the ac form. As a combination of battery and SC, HESS is more suitable for MEA than any other combination of ESDs because it takes advantage of the high energy density of battery and the high power density of SC. The power loads include all the MEA electrical loads in both ac and dc forms with power converters connected to the buses.

Here, power management is executed in the MEA controller, which aims to minimize the fluctuation of the output power from the main generators so that the system is more stable, more reliable, and more efficient. The MEA controller achieves this goal through adaptive power allocation between the power loads and different power sources main, including generators, battery, and SC, where the main generator provides the average power with slow dynamics, SC is mainly responsible for pulse power absorption, and the battery functions as a power buffer to guarantee the balance of power. Power transmission between the sources is also considered. Without loss of generality, we consider the power management in MEA as a time-slotted process in this article. The time slot duration is determined by the timescale of power generation and demand processes in the MEA.

1) ESS Model: In MEA HESS, we consider K ESDs in total, with K_1 batteries and K_2 SCs, and $K = K_1 + K_2$. Similar to some previous works [30], we assume no power loss during charging or discharging at all the ESDs, as well as a negligible leaking rate, which is a reasonable assumption since the leaking loss under the time scale in MEA power management (usually less than 1 h) is usually negligible [30].

Let $R_k(t)$ and $D_k(t)$ denote the recharging and discharging powers for ESD k in time slot t, respectively. Within any time slot t, $R_k(t)$ and $D_k(t)$ are limited by their peak values, respectively, as

$$\begin{cases} 0 \le R_k(t) \le R_{k,\max} & \forall k, t \\ 0 \le D_k(t) \le D_{k,\max} & \forall k, t. \end{cases} \tag{1}$$

Since the charging and discharging operations cannot be performed at the same time, we have

$$\begin{cases} R_k(t) > 0 \Rightarrow D_k(t) = 0 & \forall k, t \\ D_k(t) > 0 \Rightarrow R_k(t) = 0 & \forall k, t. \end{cases} \tag{2}$$

Let $E_k(t)$ be the energy level of ESD k in time slot t. The dynamics of $E_k(t)$ over time can be described as

$$E_k(t+1) = E_k(t) + \eta_{k,r} R_k(t) - \eta_{k,d} D_k(t) \quad \forall k, t \tag{3}$$

where $\eta_{k,r} < 1$ is the charging efficiency coefficient of ESD k, and $\eta_{k,d} > 1$ is the discharging efficiency coefficient of ESD k [31]. Note that the time difference of $t+1$ and t is the duration of one time slot, whose length is different according to the applications. Because of the ESD efficiency, generally, the actual stored energy through charging is less than $R_k(t)$, and the actual contributed energy through discharging is larger than $D_k(t)$.

Let $E_{k,\max}$ be the maximum capacity of ESD k, and thus, we have $E_k(t) \le E_{k,\max}$ for all t. Furthermore, for deep discharging protection, a minimum capacity $E_{k,\min} \ge 0$ is required for all time slots. Therefore, $E_k(t)$ is bounded as

$$E_{k,\min} \le E_k(t) \le E_{k,\max} \quad \forall k, t. \tag{4}$$

In each time slot t, $R_k(t)$ and $D_k(t)$ are determined under constraint (4).

2) Power Generation and Balance: Here, we mainly discuss the MEA flight conditions where the emergency generators (EMY) and auxiliary power units (APUs) do not provide power output. Thus, we consider a generator unit with N main generators. For generator i, $i \in \{1, 2, \ldots, N\}$, we have

$$P^G_{i,\min} \le P^G_i(t) \le P^G_{i,\max} \quad \forall i, t \tag{5}$$

where $P^G_i(t)$ is the output power, and $P^G_{i,\min}$ and $P^G_{i,\max}$ are the corresponding minimum and maximum power generation, respectively.

In order to balance the power supply and demand, we have

$$\sum_{i=1}^{N} P^G_i(t) + \sum_{k=1}^{K} (D_k(t) - R_k(t)) = P^L(t) \quad \forall t, \tag{6}$$

where $P^L(t)$ is the total MEA load demand.

B. Problem Formulation

As mentioned in Section I, frequent fluctuations of generator output power may increase the fuel consumption and cause instability of the MEA electrical power system [26]. Thus, we formulate a problem to minimize the fluctuations of generator output power as follows:

$$\begin{aligned} \min:\ & \lim_{t\to\infty} \frac{1}{t} \sum_{\tau=0}^{t-1} \mathbb{E}\left\{ \sum_{i=1}^{n} \left| P^G_i(\tau) - P^G_i(\tau-1) \right| \right\} \\ \text{s.t:}\ & (1), (2), (3), (4), (5), (6). \end{aligned} \tag{7}$$

There are two implicit integer variables, taken as 0 or 1, in constraint (2) to represent the charging or the discharge operation, and they cannot be 1 at the same time. Therefore, problem (7) is actually as a stochastic mixed integer linear programming problem. Traditional dynamic programming approaches can be used to solve the problem but require all possible combinations of the stored energy levels and the system states to obtain the optimal solution [33]. However, in (7), the power demand is random, and the solution also depends on the evolution of energy storage state. Therefore, we apply the Lyapunov optimization method to solve this problem by introducing virtual queues.

1) Virtual Queue: We first define a virtual queue $X_k(t)$ to track the charging level of each ESD k as follows.

$$X_k(t+1) = X_k(t) + \eta_{k,r} R_k(t) - \eta_{k,d} D_k(t) \quad \forall k, t. \tag{8}$$

By (8), $X_k(t)$ accumulates the total charging/discharging amount. Comparing (8) and (3), it can be seen that the virtual queue $X_k(t)$ and the power level $E_k(t)$ update according to the same manner. We further relate them by initializing $X_k(0) = E_k(0) - \beta_k$,where β_k is a shifting parameter, and we have

$$\beta_k = \eta_{k,d} D_{k,\max} + E_{k,\min} - V \sum_{i=1}^{n} P_{i,\min}^{G} \quad \forall k \tag{9}$$

where V is a constant for the tradeoff between the algorithm performance and the ESDs constraints, which is limited by $0 < V \leq V_{\max} = \min_k\{(E_{k,\max} - E_{k,\min} - \eta_{k,d} D_{k,\max} - \eta_{k,r} R_{k,\max}/\sum_{i=1}^{N}(P_{i,\max}^{G} - P_{i,\min}^{G}))\}$. V needs to be carefully selected to satisfy constraint (4). Actually, $X_k(t)$ is simply a shifted time series of $E_k(t)$. Unlike the actual $E_k(t)$, $X_k(t)$ may be positive or negative because of its virtuality; however, the values of $X_k(t)$ are all positive here because the capacity of ESD k is much larger than it is charging or discharging amount in a time slot (usually several seconds).

Then, we can further derive the SOC of the ESDs in time slot t as

$$\mathrm{SOC}_k(t) = \frac{X_k(t) + \beta_k}{E_{k,\mathrm{cap}}} \quad \forall k, t, \tag{10}$$

where $E_{k,\mathrm{cap}}$ is the capacity of ESD k.

2) Problem Reformulation: By introducing energy storage virtual queues, we can transform the original problem (7) into a queue stability problem, which leads to a system stability design from the perspective of control theory. Constraint (4) on ESDs is then transformed to the stability of the virtual queues, indicated by the boundness of the Lyapunov drift [defined in (13)]. The stochastic programming problem (7) can be, thus, reformulated as

$$\begin{aligned} &\min \lim_{t\to\infty} \frac{1}{t} \sum_{\tau=0}^{t-1} \mathbb{E}\left\{ \sum_{i=1}^{n} \left| P_i^G(\tau) - P_i^G(\tau-1) \right| \right\} \\ &\text{s.t. (1), (2), (5), (6)} \\ &\qquad \text{stability of all virtual queues } X_k(t). \end{aligned} \tag{11}$$

We then apply the Lyapunov optimization to design an adaptive control policy. It transforms problem (11) into several subproblems, which can be solved in every time t, and guarantees the stability of the system.

C. Lyapunov Optimization

We define the Lyapunov function for system state $\mathbf{X}(t) = \{X_1(t), \ldots, X_K(t)\}$ as

$$L(\mathbf{X}(t)) = \frac{1}{2} \sum_{k=1}^{K} [X_k(t)]^2 \tag{12}$$

which indicates the level of the stored power in the entire system at time t. $L(\mathbf{X}(t))$ actually represents the total energy included in the system. For positive $X_k(t)$, $L(\mathbf{X}(t))$ being small means that the power storage of all ESDs is low, while $L(\mathbf{X}(t))$ being large means that at least some ESDs have high level of power storage. We further define the conditional one time slot Lyapunov drift as

$$\Delta(\mathbf{X}(t)) = \mathbb{E}\{L(\mathbf{X}(t+1)) - L(\mathbf{X}(t)) | \mathbf{X}(t)\}. \tag{13}$$

The Lyapunov drift indicates the change of the system power storage in one time slot, so it is always bounded in practical systems. The following lemma provides this basic property of the Lyapunov drift.

Lemma 1: The Lyapunov drift satisfies the following inequality for all time:

$$\Delta(\mathbf{X}(t)) \leq B + \sum_{k=1}^{K} \mathbb{E}\{X_k(t)(\eta_{k,r} R_k(t) - \eta_{k,d} D_k(t)) | X_k(t)\} \tag{14}$$

where $B = (1/2)\sum_{k=1}^{K}(\max\{(\eta_{k,r} R_{k,\max})^2, (\eta_{k,d} D_{k,\max})^2\})$.

Proof: From the the virtual queues dynamics (8) and the Lyapunov function (12), we can obtain

$$\begin{aligned} \Delta(\mathbf{X}(t)) &= \frac{1}{2}\mathbb{E}\left\{ \sum_{k=1}^{K} [(X_k(t+1))^2 - (X_k(t))^2] \right\} \\ &= \mathbb{E}\left\{ \sum_{k=1}^{K} \left[\frac{1}{2}(\eta_{k,r} R_k(t) - \eta_{k,d} D_k(t))^2 \right.\right. \\ &\qquad \left.\left. + X_k(t)(\eta_{k,r} R_k(t) - \eta_{k,d} D_k(t)) | X_k(t) \right] \right\} \\ &\leq \mathbb{E}\left\{ \sum_{k=1}^{K} \left[\frac{1}{2} \max\{(\eta_{k,r} R_{k,\max})^2, (\eta_{k,d} D_{k,\max})^2\} \right.\right. \\ &\qquad \left.\left. + X_k(t)(\eta_{k,r} R_k(t) - \eta_{k,d} D_k(t)) | X_k(t) \right] \right\} \end{aligned}$$

and (14) directly follows. ∎

Here, we can minimize the drift $\Delta(\mathbf{X}(t))$ to achieve a better system performance on stability. However, our original objective is the minimization of the fluctuations of generator output power. Therefore, we add a penalty term to the drift to construct the drift-plus-penalty as $\Delta(\mathbf{X}(t)) + V\mathbb{E}\{\sum_{i=1}^{n} |P_i^G(t) - P_i^G(t-1)| | \mathbf{X}(t)\}$, where V is the constant defined in (9), used here as a weight to balance $\Delta(\mathbf{X}(t))$ and $\mathbb{E}\{\sum_{i=1}^{n} |P_i^G(t) - P_i^G(t-1)| | \mathbf{X}(t)\}$. Thus, it includes both the system stability and the fluctuations of generator output power. However, minimization of the drift-plus-penalty is a challenging optimization problem, which is difficult to

solve [28]. Fortunately, we can quickly obtain the upper bound of the drift-plus-penalty from Lemma 1

$$\begin{aligned}&\Delta(\mathbf{X}(t)) + V\mathbb{E}\left\{\sum_{i=1}^{n}\left|P_i^G(t) - P_i^G(t-1)\right||\mathbf{X}(t)\right\}\\ &\le B + \sum_{k=1}^{K} X_k(t)(\eta_{k,r}R_k(t) - \eta_{k,d}D_k(t))|X_k(t)\\ &\quad + V\mathbb{E}\left\{\sum_{i=1}^{n}\left|P_i^G(t) - P_i^G(t-1)\right||\mathbf{X}(t)\right\}. \end{aligned} \tag{15}$$

Then, we can minimize the upper bound to obtain a solution very close to the optimum. Thus, we derive the following optimization problem:

$$\begin{aligned}\min\ & B + \sum_{k=1}^{K} X_k(t)(\eta_{k,r}R_k(t) - \eta_{k,d}D_k(t))\\ &+ V\sum_{i=1}^{n}\left|P_i^G(t) - P_i^G(t-1)\right|\\ \text{s.t:}\ & (1), (2), (5), (6)\end{aligned} \tag{16}$$

which can be solved based on the current observation so that the conditional probability on $X_k(t)$ is removed. The constraint on the virtual queues $X_k(t)$ in (11) is combined in the objective function of (16). This way, problem (11) for the entire time period is decomposed into a series of subproblems (16), one for each time slot t, which can be solved in an online manner. We then show the boundedness of virtual queues $X_k(t)$ and actual queues $E_k(t)$ and present the relationship between the solutions to (16) and the original problem (7).

III. Online Solutions

Based on the Lyapunov drift-plus-penalty method, we successfully transform problem (7)–(16) to be solved online in each time slot. Before discussing the online solutions, we first present the following constraint of $X_k(t)$ on the charging power $R_k(t)$ and discharging power $D_k(t)$.

Lemma 2: For any initial value $X_k(0)$, the charging power $R_k(t)$ and discharging power $D_k(t)$ satisfy the following.

1) If $X_k(t) > V\sum_{i=1}^{N} P_{i,\max}^G$, ESD k cannot be charged, i.e., $R_k(t) = 0$.
2) If $X_k(t) < V\sum_{i=1}^{N} P_{i,\min}^G$, ESD k cannot be discharged, i.e., $D_k(t) = 0$.

Lemma 2 provides two thresholds for $X_k(t)$. At each time slot t, if $X_k(t)$ is higher than the upper threshold, the charging amount for ESD k is zero, so $X_k(t+1)$ cannot be increased at $t+1$. Similarly, if $X_k(t)$ is smaller than the lower threshold, the discharging amount for the ESD k is zero, and $X_k(t+1)$ cannot be decreased during slot $t+1$. Therefore, ESDs could work more effectively and efficiently. We further present the bounds of $X_k(t)$ and $E_k(t)$ for the online solutions to (16).

Lemma 3: Let $g(t) = P^L(t) - \sum_{i=1}^{N} P_i^G(t-1)$, charging/discharging for ESD k in time slot t is restricted by the following.

1) If $g(t) > 0$, ESD k cannot be charged, i.e., $R_k(t) = 0$.
2) If $g(t) < 0$, ESD k cannot be discharged, i.e., $D_k(t) = 0$.

Lemma 3 indicates that when the load demand at time t is beyond the total power output of $t-1$, ESDs are not allowed to increase the load burden, and the decision variables in problem (16) are $P_i^G(t)$ and $D_k(t)$; when the load demand is less than the total power output, the MEA power system needs no power from the ESDs, and the decision variables in problem (16) are turned into $P_i^G(t)$ and $R_k(t)$. In this way, problem (16) is solved as a linear programming problem. This is actually conforming to the optimal solutions in most cases. However, we use Lemma 3 to avoid the worst case and also simplify the algorithm design.

Theorem 1: Given the initial energy storage level $X_k(0) = E_k(0) - \beta_k$, the virtual queue $X_k(t)$ is bounded within $[E_{k,\min} - \beta_k, E_{k,\max} - \beta_k]$ for all k and t.

Proof: Assuming that the inequalities hold true for time t, we then demonstrate that the inequalities still hold true for time $t+1$, i.e., $E_{k,\min} - \beta_k \le X_k(t+1) \le E_{k,\max} - \beta_k$.

We first prove the upper bound $X_k(t+1) \le E_{k,\max} - \beta_k$. Consider the following two cases.

Case 1: $V\sum_{i=1}^{N} P_{i,\max}^G < X_k(t) \le E_{k,\max} - \beta_k$. From Lemma 2, we have $R_k(t) = 0$ for $X_k(t) > V\sum_{i=1}^{N} P_{i,\max}^G$, and from (8), we have $X_k(t+1) = X_k(t) - \eta_{k,d}D_k(t) \le X_k(t) \le E_{k,\max} - \beta_k$.

Case 2: $X_k(t) \le V\sum_{i=1}^{N} P_{i,\max}^G$. From (8), the largest value of $X_k(t+1)$ is, thus, $V\sum_{i=1}^{N} P_{i,\max}^G + \eta_{k,r}R_{k,\max}$. Thus, for any $0 \le V \le V_{\max}$, we have

$$\begin{aligned}&E_{k,\max} - \beta_k - \left(V\sum_{i=1}^{N} P_{i,\max}^G + \eta_{k,r}R_{k,\max}\right)\\ &\ge E_{k,\max} - \eta_{k,d}D_{k,\max} - E_{k,\min} - \eta_{k,r}R_{k,\max}\\ &\quad - \min_k\left\{\frac{E_{k,\max} - E_{k,\min} - \eta_{k,d}D_{k,\max} - \eta_{k,r}R_{k,\max}}{\sum_{i=1}^{N}\left(P_{i,\max}^G - P_{i,\min}^G\right)}\right\}\\ &\quad \cdot \sum_{i=1}^{N}\left(P_{i,\max}^G - P_{i,\min}^G\right) \ge 0.\end{aligned}$$

Therefore, $X_k(t+1) \le E_{k,\max} - \beta_k$ holds true for both cases. We then prove the lower bound. Supposing that $X_k(t) \ge E_{k,\min} - \beta_k$ is true, we also consider the following two cases.

Case 1: $E_{k,\min} - \beta_k \le X_k(t) < V\sum_{i=1}^{N} P_{i,\min}^G$. From Lemma 2, we have $D_k(t) = 0$ for $X_k(t) < V\sum_{i=1}^{N} P_{i,\min}^G$. Then, from (8), we have $X_k(t+1) = X_k(t) + \eta_{k,r}R_k(t) \ge X_k(t) \ge E_{k,\min} - \beta_k$.

Case 2: $X_k(t) \ge V\sum_{i=1}^{N} P_{i,\min}^G$. From (8), we have $X_k(t+1) = X_k(t) - \eta_{k,d}D_k(t) + \eta_{k,r}R_k(t) \ge X_k(t) - \eta_{k,d}D_{k,\max} \ge E_{k,\min} - \beta_k$.

Thus, $X_k(t+1) \ge E_{k,\min} - \beta_k$ also holds true for both cases. Therefore, we have that $E_{k,\min} - \beta_k \le X_k(t+1) \le E_{k,\max} - \beta_k$ holds true for time slot $t+1$. ∎

By Theorem 1, we can quickly acquire Theorem 2 (proof is omitted for the limit of space) on the boundedness of the actual energy queues $E_k(t)$ and further propose Theorem 3 about the online solutions.

Theorem 2: Given the initial energy storage level $E_k(0) = X_k(0) + \beta_k$, the actual energy queue $E_k(t)$ is bounded within $[E_{k,\min}, E_{k,\max}]$ for all k and t.

Theorem 3: The average variation of the generator output power under the online solutions to problem (16), denoted by f^*, is bounded as $f^* \le f^{\text{opt}} + B/V$, where f^{opt} is the optimal solution to problem (7).

Proof: From Theorems 1 and 2, the virtual queue $X_k(t)$ and the actual energy queue $E_k(t)$ are all bounded. Take expectation on (3) and sum it over the period $[0, t-1]$, we have

$$\mathbb{E}\{E_k(t)\} - \mathbb{E}\{E_k(0)\} = \sum_{\tau=0}^{t-1} [\eta_{k,r}\mathbb{E}\{R_k(\tau)\} - \eta_{k,d}\mathbb{E}\{D_k(\tau)\}] \quad \forall k.$$

Since $E_{k,\min} \le E_k(t) \le E_{k,\max}$, we divide both sides of the equation by t, and let t go to infinity, to have

$$\eta_{k,r} \lim \frac{1}{t}\sum_{\tau=0}^{t-1} \mathbb{E}\{R_k(\tau)\} = \eta_{k,d} \lim \frac{1}{t}\sum_{\tau=0}^{t-1} \mathbb{E}\{D_k(\tau)\} \quad \forall k. \quad (17)$$

Now, we consider a relaxed problem of (7) by replacing constraint (3) by (17)

$$\begin{aligned} \min \ & \lim_{t\to\infty} \frac{1}{t}\sum_{\tau=0}^{t-1} \mathbb{E}\left\{\sum_{i=1}^{n} \left| P_i^G(\tau) - P_i^G(\tau-1)\right|\right\} \\ \text{s.t:} \ & (1), (2), (3), (5), (6), (17). \end{aligned} \quad (18)$$

Since constraint (3) is relaxed by (17), the optimal solutions to (7) are also feasible for (18), but the solutions to (18) do not depend on the energy levels of the ESDs. Let $\hat{\mathbb{A}}(t) = \{\hat{P}_i^G(t), \hat{R}_k(t), \hat{D}_k(t)\}$ denote the optimal solutions to (18) and $\hat{f}$ denote the corresponding optimal objective value, which is less than or equal to f^{opt}. Therefore, the optimal solution $\hat{\mathbb{A}}(t)$ satisfies $\mathbb{E}\{\eta_{k,r}\hat{R}_k(t) - \eta_{k,d}\hat{D}_k(t)\} = 0$ and $\hat{f} = \mathbb{E}\{\sum_{i=1}^{n} \left| P_i^{\hat{G}}(\tau) - P_i^G(\hat{\tau}-1)\right|\}$.

Since problem (16) originally minimizes the right-hand side of the drift-and-penalty (15), we have

$$\begin{aligned} &\Delta(\mathbf{X}(t)) + V\mathbb{E}\left\{\sum_{i=1}^{n}\left|P_i^G(\tau) - P_i^G(\tau-1)\right| | \mathbf{X}(t)\right\} \\ &\le B + \sum_{k=1}^{K} \mathbb{E}\{X_k(t)(\eta_{k,r}\hat{R}_k(t) - \eta_{k,d}\hat{D}_k(t)) | X_k(t)\} \\ &\quad + V\mathbb{E}\left\{\sum_{i=1}^{n}\left|\hat{P}_i^G(\tau) - \hat{P}_i^G(\tau-1)\right| | \mathbf{X}(t)\right\} \\ &\le B + V \cdot f^{\text{opt}} \end{aligned}$$

which holds because $\mathbb{E}\{\eta_{k,r}\hat{R}_k(t) - \eta_{k,d}\hat{D}_k(t)\} = 0$ and $\hat{f} < f^{\text{opt}}$. Taking expectation and summing up from 0 to $T-1$, we obtain

$$\begin{aligned} &\sum_{t=0}^{T-1} V\mathbb{E}\left\{\sum_{i=1}^{n}\left|P_i^G(\tau) - P_i^G(\tau-1)\right|\right\} \\ &\quad \le T\cdot B + T\cdot V\cdot f^{\text{opt}} + \mathbb{E}\{L(\mathbf{X}(0))\} - \mathbb{E}\{L(\mathbf{X}(T))\} \\ &\quad \le T\cdot B + T\cdot V\cdot f^{\text{opt}} + \mathbb{E}\{L(\mathbf{X}(0))\}. \end{aligned}$$

Dividing both sides by VT and letting T go to infinity, we have

$$\lim_{T\to\infty}\frac{1}{T}\sum_{t=0}^{T-1} V\mathbb{E}\left\{\sum_{i=1}^{n}\left|P_i^G(\tau) - P_i^G(\tau-1)\right|\right\} \le f^{\text{opt}} + \frac{B}{V}$$

assuming that the initial system state is finite. ■

Algorithm 1: OPMA for the MEA Controller

1 **Initialize:** the output power $P_i^G(t)$ of the generators, the virtual queues $X_k(t)$, and $\text{SOC}_k(t)$ for all i and k;
2 **while** $t \le T$ **do**
3 Read the current system state: $X_k(t)$, $\text{SOC}_k(t)$, $P_i^G(t-1)$, $P^L(t)$;
4 Obtain the optimal solution $\mathbb{A}(t)$ by solving Problem (16) with Lemmas 2 and 3;
5 Update the virtual queues $X_k(t)$ according to (8) and calculate $\text{SOC}_k(t)$, for all k;
6 $t \leftarrow t+1$;
7 **end while**

From Theorem 3, the optimal objective value of (16) is away from that of (7) by $O(1/V)$, and thus, a larger V leads to a better performance of the proposed algorithm, i.e., a smaller optimality gap. However, from Lemma 2, V is limited by $V_{\max}$ to ensure that constraints (4) are satisfied. Through the definition of $V_{\max}$, it can achieve a better performance if more ESS capacity is configured. In addition, all the constraints are deterministic, and the proposed method, thus, provides an online power management approach for MEA, considering both the variation of generator output power and system stability.

IV. AOPM FOR MEA

Based on the theoretical results, we further propose the AOPM for MEA in this section.

A. Online Power Management Algorithm

According to the online solutions in Section III, we present the online power management algorithm (OPMA) for MEA controller in Algorithm 1, which only requires the current observation of system state, without the knowledge of the statistical load information. First, the MEA controller initializes the output power $P_i^G(t)$ of all generators and all virtual queues $X_k(t)$ and $\text{SOC}_k(t)$.[1] In each time slot t, the MEA controller observes the current virtual queues $X_k(t)$, state-of-charge $\text{SOC}_k(t)$, and output power $P_i^G(t-1)$ of the generators of the previous time slot $t-1$ and the total MEA load $P^L(t)$ for all i and k. Then, the MEA controller derives the optimal solution $\mathbb{A}(t)$ by solving problem (16) under the restrictions in Lemmas 2 and 3. The MEA controller then obtains the current output power $P_i^G(t)$ of the generators, the charging amount $R_k(t)$, and discharging amount $D_k(t)$ for HESS. Finally, the MEA controller updates the virtual queues $X_k(t)$ according to (8) and calculates the state-of-charge $\text{SOC}_k(t)$. Besides, the proposed algorithm needs to repeat T times loop for the whole operation from steps 3–6 until the last time slot. In step 4, the optimal solution $\mathbb{A}(t)$ is calculated by solving linear programming problem using an LP solver with complexity $\mathcal{O}(n\log(n))$ [34]. For Algorithm 1,

[1]Note that the solutions are not sensitive to the variations in initial conditions [28].

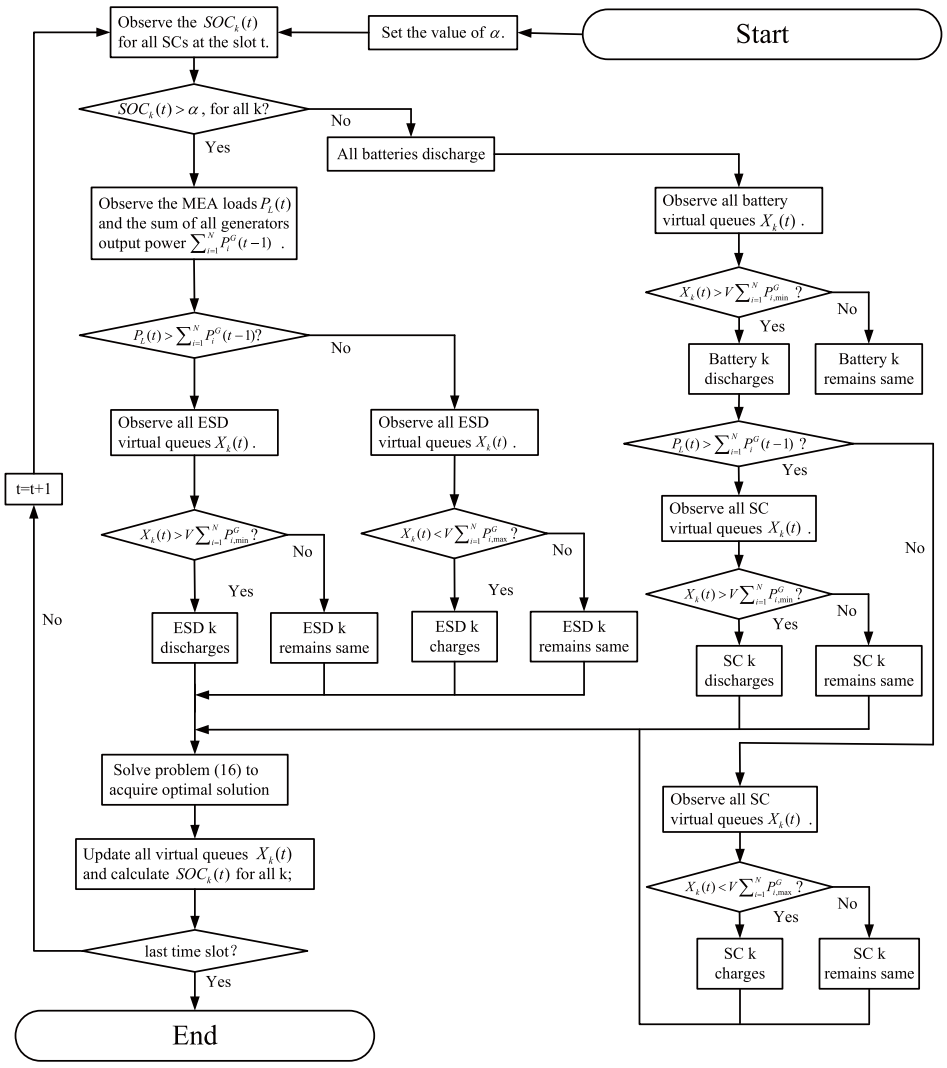

Fig. 2. Flowchart of AOPM.

T is a constant, so the running time of our algorithm can be obtained, which is recorded as $T(\mathcal{O}(n\log(n)))$.

B. AOPM

OPMA is able to smooth the fluctuation of the power output of main generators in most flight phases. However, nonlinear large power load pulses are the real challenges to power management in MEA. Usually, SCs are expected to absorb instantaneous power peaks. Our solution is to use batteries to charge SCs when SC's SOC is low. However, the weight of HESS has to be considered as well. It is, thus, important to make full use of the ESDs according to their characteristics to optimize the total weight of ESDs as much as possible.

Motivated by this, we design a control strategy to discharge the SCs to absorb large load pulses and then recharge the SCs by batteries, while the OPMA does not control batteries to charge SCs. This is especially important in some fighter planes using weapons of high power density, such as lasers, which has very large power demands, e.g., nearly ten times the average power [19]. Also, this may occur in some emergency situations. Actually, batteries are used here as energy buffers between the main generators and SCs, which balances the capacity of load smoothing and the weight of HESS. The control strategy is summarized in Strategy 1. Note that the parameter α is set as the charging alert of the SC, which triggers the charging from batteries to SCs. A bigger α indicates more frequent battery discharging as the trigger is easier to be reached, while smaller α increases the time of the SC being a low level of SOC such that the sudden power peaks may not be fully absorbed. Thus, α needs to be carefully selected, considering the tradeoff between less battery charging and more power storage in SC.

Strategy 1: Set parameter α, and determine the value of SOC of every SC k, denoted as $\mathrm{SOC}_k(t)$. If any $\mathrm{SOC}_k(t)$ is less than α, all batteries discharge.

Combining strategy 1 and OPMA, we propose the AOPM for MEA, which is summarized in Fig. 2. AOPM can be used to smooth the power output of the main generators in different flight phases in an adaptive online manner.

V. Simulation Studies

A. System Descriptions

In order to demonstrate the effectiveness of the proposed OPMA and AOPM for MEA, we simulate the MEA power

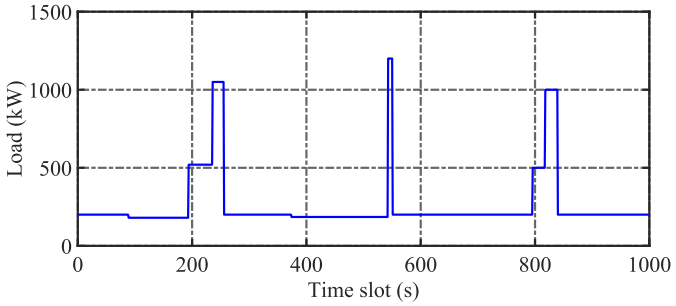

Fig. 3. MEA load with large instantaneous power pulses.

system according to the structure in Fig. 1. The maximum and minimum output powers for the main generator are assumed to be 1000 and 50 kW, respectively [2]. The capacity of the battery is set to 100 kWh. The maximum energy storage for the battery is 80 kWh, and the minimum is 20 kWh. The corresponding SOC range is $[0.2, 0.8]$, and the charging and discharging efficiency coefficients are 0.9 and 1.1. Similarly, the capacity of the SC is set to 10 kWh. The maximum and minimum levels for the SC are 9 and 1 kWh, respectively, and the corresponding SOC range is $[0.1, 0.9]$. The charging and discharging efficiency coefficients are 0.98 and 1.02. The maximum charging/discharging power is 200 kW for the battery and 3500 kW for the SC [26], [35].

As previously discussed, the most challenging power management for MEA happens when the system needs to support large output power, especially the instantaneous large power pulses. Therefore, we mainly focus on the simulations to evaluate the capability of the proposed AOPM to stabilize the power fluctuations of the generators in cases when several power pulses of the loads occur. The load curve shown in Fig. 3 is taken from a real flight trace of a fighter aircraft. The time interval is set to 1 s. The control parameter is $V = V_{\max}$, unless otherwise stated. The initial SOCs of HESS are both 0.5, and the initial generator output power is 220 kW. In the realization of our proposed power management methods, we use the MATLAB LP solver to solve problem (16).

B. Performance of OPMA

We first present the average generator output power, SOC of battery, and SOC of SC under OPMA in Fig. 4. Comparing Fig. 4(a) with Fig. 3, we can see that the power pulse occurs when $t = 526$ s has been absorbed, and the power peaks when $t = 195$ s and $t = 798$ s are greatly weakened but still exist in the power output of the generator. The SC is mainly responsible for the power peak absorption. The first and the third power peaks are too large for the SC to absorb. Also, in OPMA, the battery does not charge the SC, so no energy buffer is constructed between the SC and the power generator such that the SC is only charged by the power generator, leading to a low SOC state throughout the entire process, especially after the first power peak. Therefore, the power generator is pushed to very high power peaks twice. For other power demands, OPMA works very well. In this situation, SC cannot fully absorb these peaks unless the initial

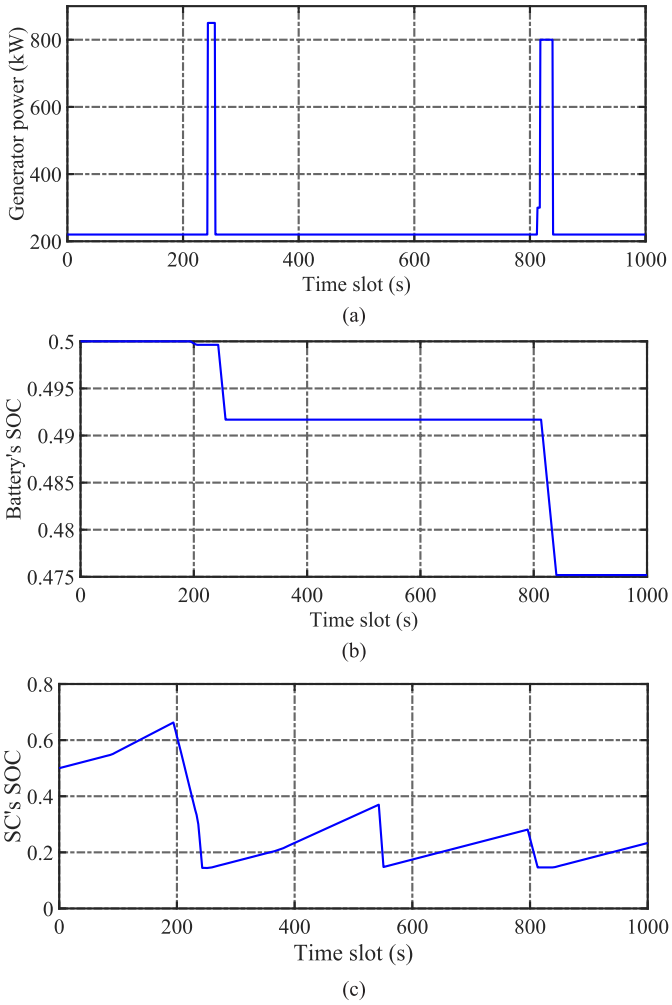

Fig. 4. Simulated power curves obtained with the proposed OPMA algorithm for MEA. (a) Average generator output power. (b) SOC of the battery. (c) SOC of the SC.

SOC of the SC or the capacity of the SC is large enough. However, the initial value of SC's SOC is uncertain in the real situation. In order to avoid burdening the weight of the aircraft, the capacity of SC should also be as small as possible. Therefore, strategy 1 is, thus, proposed to deal with such situations.

C. Performance of AOPM

Now, we evaluate AOPM for the same power load in Fig. 3. We plot the average generator output power, SOC of battery, and SOC of SC under OPMA and AOPM under different α's in Fig. 5. The parameter α triggers the charging from batteries to SCs. A larger α indicates more frequent battery discharging as the trigger is more easily reached, while smaller α increases the time duration of the SC being a lower level of SOC such that the sudden power peaks may not be fully absorbed. We can see that when $\alpha = 0.5$, the capacity of the SC has reached the lower bound before the end of the load power peaks. When $\alpha = 0.9$, the battery is working (either charging or discharging) all the time, which is bad for battery life. This is also unnecessary because the generator has to

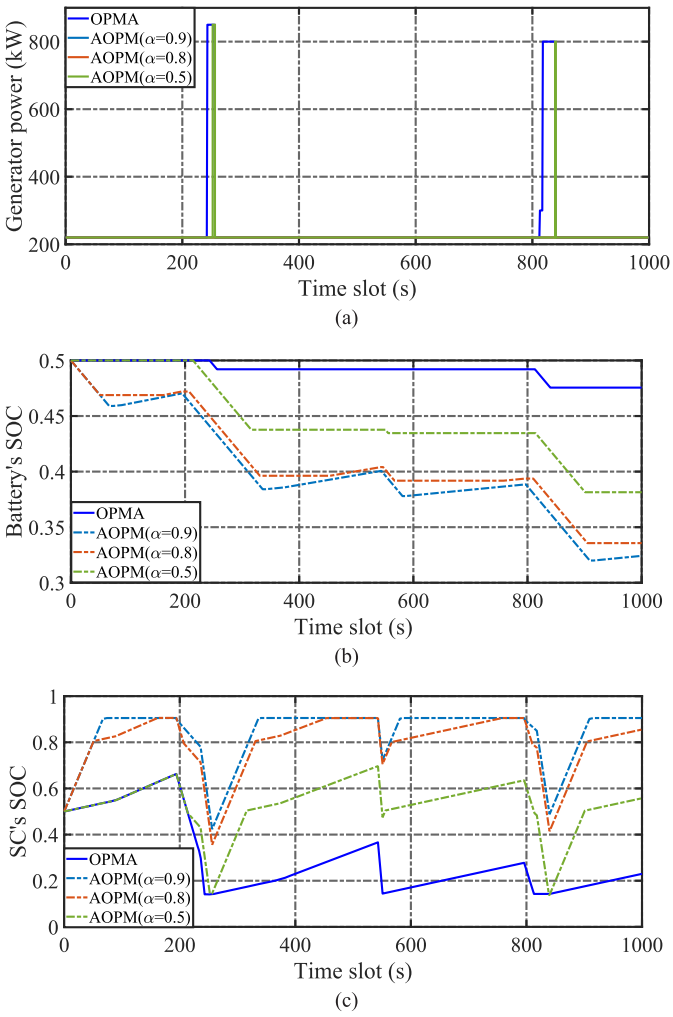

Fig. 5. Simulated power curves obtained with the proposed OPMA and AOPM algorithms under different α values. (a) Average generator output power. (b) SOC of battery. (c) SOC of SC.

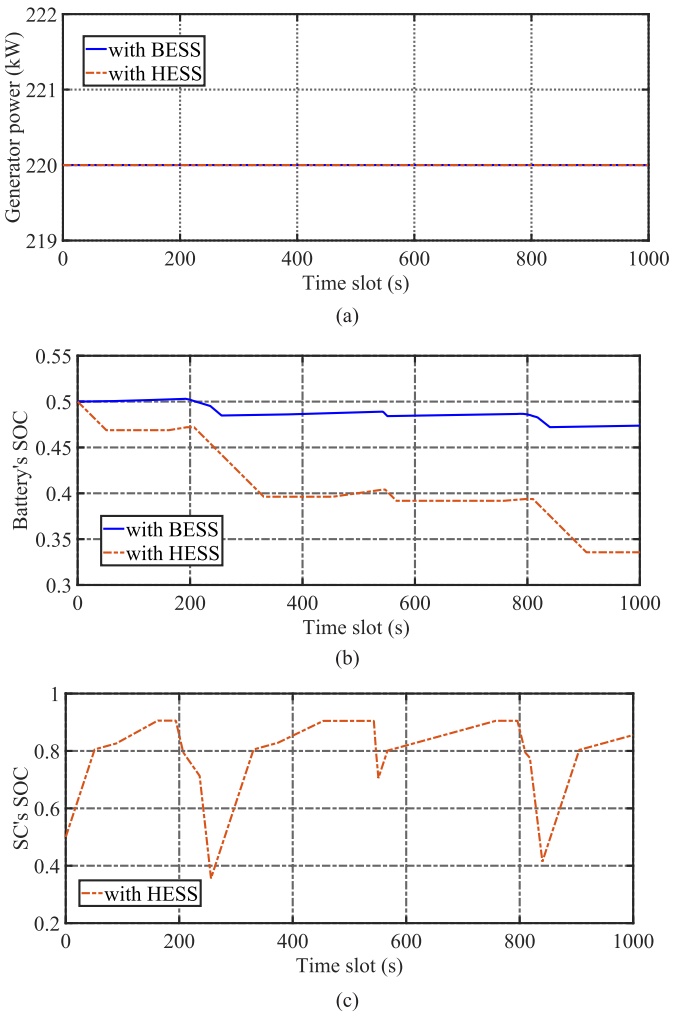

Fig. 6. Simulated power curves with different HESS configurations. (a) Average generator output power. (b) SOC of battery. (c) SOC of SC.

charge the SC sometimes. Therefore, 0.8 is a more appropriate value in case of the situation with higher and longer load power peaks.

Now, we compare the performance of AOPM and OPMA with α set as 0.8. We can see that comparing with OPMA, the power output from the generator under AOPM is quite smooth with no power peaks. This is because batteries are controlled to charge SCs so that the HESS is able to absorb large power pulses of the load. With AOPM, it is clear from Fig. 5(b) and (c) that after each power pulse of the load, the SC discharges deeply, and then, the batteries charge the SC until its SOC goes up and back to $\alpha = 0.8$. For example, the battery remains discharging until $t = 51$ s, during which the SC keeps charging. At $t = 51$ s, SC's SOC reaches 0.8; at that point, the battery no longer discharges. Since the power supplied by the generator is more than the power demand, the SC remains in the state of charging, and the battery keeps unchanged. The results in Fig. 4 illustrate that AOPM performs better than OPMA in smoothing the power leaks of the load, which verifies the effectiveness of strategy 1. This also provides the possibility to reduce the main generator's capacity configuration, by reducing the required capability of the generator for the overload correspondingly.

D. Comparisons Between Different HESS Configurations

We now change the configurations of battery and SC in the system and compare different HESS combinations. In previous evaluations, the capacities of battery and SC are set to 100 and 10 kWh, respectively. From Fig. 5(c), we notice that the lowest point of the SC is 0.35, which is much higher than its lower limit 0.1, but the highest point is close to the upper limit 0.9. Therefore, we can reduce the capacity of the battery to approach the HESS's operating limit. Based on the load in Fig. 3, the capacity of the battery can be reduced to 29 kWh, but it can still smooth the power output of the generator under AOPM. On the other hand, we try to smooth the power output under pure BESS without SC, with the same charging/discharging power of 200 kW. In this case, without the capability of instantaneous power output, the capacity of the battery has to be increased from 100 to 490 kWh. Besides, the parameter α is set to 0.8 here.

We list the major parameters of the two configurations in Table I and plot the corresponding power curves with AOPM in Fig. 6. From the table and figures, it can be seen

TABLE I
RESULTS UNDER DIFFERENT ENERGY STORAGE MODELS

Energy storage model	BESS	HESS
Battery specific power (kW)	980	58
Battery specific energy (kWh)	490	29
Supercapacitor specific power (kW)	–	3500
Supercapacitor specific energy (kWh)	–	10

that the power output of the generator can still be smoothed using AOPM under these two capacity configurations, and the new HESS configuration makes full use of the SCs. Also, the pure BESS scheme is not applicable because it adds large extra weights, about 300–1000 kg [35]. The specific powers are between 120 and 140 Wh/kg for the batteries and 5 and 15 Wh/kg for the SCs [26]. Therefore, we conclude that HESS consisting of both SCs and batteries is necessary for the MEA, and AOPM can fully utilize the HESS with very high efficiency.

VI. CONCLUSION

In this article, we first developed an MEA power management model based on HESS aiming to minimize the generator output power fluctuation. The battery–SC HESS was used as a temporary energy buffer to cope with the load peaks, leading to a smooth output of the generator. We then developed the Lyapunov optimization method and transformed the ESS management problem into a queue stability problem by introducing energy storage virtual queues. By integrating a control strategy with the Lyapunov optimization method, we proposed the AOPM for MEA, which was able to deal with the load pulses. The feasibility and adaptivity of the proposed method were validated with trace-driven simulations.

REFERENCES

[1] B. Sarlioglu and C. T. Morris, "More electric aircraft: Review, challenges, and opportunities for commercial transport aircraft," *IEEE Trans. Transport. Electrific.*, vol. 1, no. 1, pp. 54–64, Jun. 2015.

[2] V. Madonna, P. Giangrande, and M. Galea, "Electrical power generation in aircraft: Review, challenges, and opportunities," *IEEE Trans. Transport. Electrific.*, vol. 4, no. 3, pp. 646–659, Sep. 2018.

[3] J. Chen, C. Wang, and J. Chen, "Investigation on the selection of electric power system architecture for future more electric aircraft," *IEEE Trans. Transport. Electrific.*, vol. 4, no. 2, pp. 563–576, Jun. 2018.

[4] W. Dunham, B. Hencey, A. R. Girard, and I. Kolmanovsky, "Distributed model predictive control for more electric aircraft subsystems operating at multiple time scales," *IEEE Trans. Control Syst. Technol.*, early access, Aug. 15, 2019, doi: 10.1109/TCST.2019.2932654.

[5] P. Nuzzo *et al.*, "A contract-based methodology for aircraft electric power system design," *IEEE Access*, vol. 2, pp. 1–25, 2014.

[6] Q. Xu, P. Wang, J. Chen, C. Wen, and M. Y. Lee, "A module-based approach for stability analysis of complex more-electric aircraft power system," *IEEE Trans. Transport. Electrific.*, vol. 3, no. 4, pp. 901–919, Dec. 2017.

[7] J. Chen and Q. Song, "A decentralized energy management strategy for a fuel cell/supercapacitor-based auxiliary power unit of a more electric aircraft," *IEEE Trans. Ind. Electron.*, vol. 66, no. 7, pp. 5736–5747, Jul. 2019.

[8] D. Schlabe and J. Lienig, "Energy management of aircraft electrical systems–state of the art and further directions," in *Proc. Electr. Syst. Aircr., Railway Ship Propuls.*, Oct. 2012, pp. 1–6.

[9] T. Schroeter and D. Schulz, "Aircraft power management–Algorithms and interactions," in *Proc. Int. Symp. Power Electron. Power Electron., Electr. Drives, Autom. Motion*, Jun. 2012, pp. 432–439.

[10] A. Barzegar *et al.*, "Intelligent power allocation and load management of more electric aircraft," in *Proc. IEEE 11th Int. Conf. Power Electron. Drive Syst.*, Jun. 2015, pp. 533–538.

[11] R. D. Telford, S. J. Galloway, and G. M. Burt, "Evaluating the reliability & availability of more-electric aircraft power systems," in *Proc. 47th Int. Universities Power Eng. Conf. (UPEC)*, Sep. 2012, pp. 1–6.

[12] X. Roboam, "New trends and challenges of electrical networks embedded in 'more electrical aircraft,"' in *Proc. IEEE Int. Symp. Ind. Electron.*, Gdansk, Poland, Jun. 2011, pp. 26–31.

[13] C. Pan, L. Chen, L. Chen, C. Huang, and M. Xie, "Research on energy management of dual energy storage system based on the simulation of urban driving schedules," *Int. J. Electr. Power Energy Syst.*, vol. 44, no. 1, pp. 37–42, Jan. 2013.

[14] S. Vazquez, S. M. Lukic, E. Galvan, L. G. Franquelo, and J. M. Carrasco, "Energy storage systems for transport and grid applications," *IEEE Trans. Ind. Electron.*, vol. 57, no. 12, pp. 3881–3895, Dec. 2010.

[15] J. Bernard *et al.*, "Fuel cell/battery passive hybrid power source for electric powertrains," *J. Power Sources*, vol. 196, no. 14, pp. 5867–5872, Jul. 2011.

[16] L. M. Fernandez, P. Garcia, C. A. Garcia, and F. Jurado, "Hybrid electric system based on fuel cell and battery and integrating a single DC/DC converter for a tramway," *Energy Convers. Manage.*, vol. 52, no. 5, pp. 2183–2192, May 2011.

[17] H. Ibrahim, A. Ilinca, and J. Perron, "Energy storage systems–Characteristics and comparisons," *Renew. Sustain. Energy Rev.*, vol. 12, no. 5, pp. 1221–1250, Jun. 2008.

[18] P. Hall and E. Bain, "Energy-storage technologiesand electricity generation," *Energy Policy*, vol. 36, no. 12, pp. 4352–4355, Oct. 2008.

[19] T. Li and D. Zhou, "Design and simulation of MEA storage system with supercapacitor," *Aeronaut. Comput. Technique*, vol. 46, no. 4, pp. 131–134, Jul. 2016.

[20] D. Zhou *et al.*, "Study on hybrid energy storage system of more electric aircraft," *Aeronaut. Comput. Technique*, vol. 46, no. 2, pp. 127–130, May 2016.

[21] M.-E. Choi, S.-W. Kim, and S.-W. Seo, "Energy management optimization in a battery/supercapacitor hybrid energy storage system," *IEEE Trans. Smart Grid*, vol. 3, no. 1, pp. 463–472, Mar. 2012.

[22] T. Zhou and W. Sun, "Optimization of battery-supercapacitor hybrid energy storage station in Wind/Solar generation system," *IEEE Trans. Sustain. Energy*, vol. 5, no. 2, pp. 408–415, Apr. 2014.

[23] A. Iovine, T. Rigaut, G. Damm, E. De Santis, and M. D. Di Benedetto, "Power management for a DC MicroGrid integrating renewables and storages," *Control Eng. Pract.*, vol. 85, pp. 59–79, Apr. 2019.

[24] C. Romaus, K. Gathmann, and J. Bocker, "Optimal energy management for a hybrid energy storage system for electric vehicles based on stochastic dynamic programming," in *Proc. IEEE Vehicle Power Propuls. Conf.*, Sep. 2010, pp. 1–6.

[25] J. Shen and A. Khaligh, "A supervisory energy management control strategy in a battery/ultracapacitor hybrid energy storage system," *IEEE Trans. Transport. Electrific.*, vol. 1, no. 3, pp. 223–231, Oct. 2015.

[26] N. Devillers, M.-C. Péra, D. Bienaimé, and M.-L. Grojo, "Influence of the energy management on the sizing of electrical energy storage systems in an aircraft," *J. Power Sources*, vol. 270, pp. 391–402, Dec. 2014.

[27] J. Li, L. Liang, S. L. Yang, and D. Hui, "Study on energy storage system smoothing wind power fluctuations," in *Proc. Int. Conf. Power Syst. Technol.*, Oct. 2010, pp. 1–4.

[28] M. Neely, *Stochastic Network Optimization With Application to Communication and Queueing Systems*. San Rafael, CA, USA: Morgan & Claypool, 2010.

[29] L. Tassiulas and A. Ephremides, "Stability properties of constrained queueing systems and scheduling policies for maximum throughput in multihop radio networks," *IEEE Trans. Autom. Control*, vol. 37, no. 12, pp. 1936–1948, Dec. 1992.

[30] L. Yang, X. Chen, J. Zhang, and H. V. Poor, "Cost-effective and privacy-preserving energy management for smart meters," *IEEE Trans. Smart Grid*, vol. 6, no. 1, pp. 486–495, Jan. 2015.

[31] S. Sun, M. Dong, and B. Liang, "Real-time power balancing in electric grids with distributed storage," *IEEE J. Sel. Topics Signal Process.*, vol. 8, no. 6, pp. 1167–1181, Dec. 2014.

[32] A. Bemporad and M. Morari, "Control of systems integrating logic, dynamics, and constraints," *Automatica*, vol. 35, no. 3, pp. 407–427, 1999.

[33] D. Bertsekas, *Dynamic Programming and Optimal Control*, vol. 2, 3rd ed. Belmont, MA, USA: Athena Scientific, 2007.
[34] S. Wright and J. Nocedal, *Numerical Optimization*. New York, NY, USA: Springer Science, 1999.
[35] L. Cheng, F. Zhang, H. Zou, and Y. Wang, "High power density optimal configuration for hybrid energy storage system based on wavelet transform," in *Proc. 21st Int. Conf. Electr. Mach. Syst. (ICEMS)*, Oct. 2018, pp. 836–840.

Yu Wang (Member, IEEE) received the B.S. and M.S. degrees in instrument science and engineering from Southeast University, Nanjing, China, in 2008 and 2011, respectively, and the Ph.D. degree in electrical and computer engineering from Auburn University, Auburn, AL, USA, in 2015.

He is currently an Assistant Professor with the Department of Electrical Engineering, Nanjing University of Aeronautics and Astronautics, Nanjing. His research interests include power management and optimization in MEA, smart grids, and microgrids.

Fang Xu received the B.E. degree in electrical engineering and automation from the Nanjing University of Aeronautics and Astronautics, Nanjing, China, in 2018, where she is currently pursuing the M.S. degree with the Department of Electrical and Computer Engineering.

Her research interests include power and energy optimization in MEA, smart grids, and microgrids.

Shiwen Mao (Fellow, IEEE) received the Ph.D. degree in electrical and computer engineering from Polytechnic University, Brooklyn, NY, USA, in 2004.

He is the Samuel Ginn Distinguished Professor and the Director of the Wireless Engineering Research and Education Center (WEREC), Auburn University, Auburn, AL, USA. His research interests include wireless networks, multimedia communications, and smart grids.

Dr. Mao received the NSF CAREER Award in 2010. He was a corecipient of the Best Demo Award from the IEEE SECON 2017, the Best Paper Awards from the IEEE GLOBECOM 2015 and 2016, the IEEE WCNC 2015, and the IEEE ICC 2013, and the 2004 IEEE Communications Society Leonard G. Abraham Prize in the field of communications systems.

Shanshui Yang (Member, IEEE) received the B.S., M.S., and Ph.D. degrees in electrical engineering from the Nanjing University of Aeronautics and Astronautics, Nanjing, China in 1991, 1994, and 2011, respectively.

He is currently an Assistant Professor with the Department of Electrical Engineering, College of Automation Engineering, Nanjing University of Aeronautics and Astronautics. His research interests include power design and modeling and management in aircraft and spacecraft.

Yinxing Shen received the B.E. degree in smart grid information engineering from the Nanjing University of Science and Technology, Nanjing China, in 2016, and the M.S. degree from the Department of Electrical and Computer Engineering, Nanjing University of Aeronautics and Astronautics, Nanjing, in 2019.

He is currently an Assistant Engineer with Ningbo Power Supply Company, Zhejiang Electric Power Corporation of State Grid, Ningbo, China.